Dr. Kam W. Wong
University of Illinois
Urbana, IL 61801

Geometric and Cartographic Accuracy of ERTS-1 Imagery

ERTS-1 RBV and MSS imagery can meet National Map Accuracy Standards for 1:500,000 scale mapping.

Abstract: *The potential application of the* **RBV** *and* **MSS** *images in cartographic mapping is limited by resolution rather than by geometric fidelity. A bulk* **RBV** *image from* **ERTS-1** *should have sufficient geometric fidelity to meet the National Map Accuracy Standards for mapping at 1:500,000 scale. With four or more control points for distortion correction, a bulk MSS frame could also be processed to meet the* **NMAS** *requirement of 1:500,000-scale mapping. In digital processing, a relative positioning accuracy of ±55m should be attainable for both* **RBV** *and* **MSS** *images. High-order polynomials were found to be very effective in modeling the total geometric distortions in both the RBV and MSS systems.*

Introduction

The first U.S. Earth Resources Technology Satellite *(ERTS-1)*, successfully launched into earth orbit on July 23, 1972, carries on board a three-camera Return-Beam-Vidicon *(RBV)* television system and a four-channel Multispectral Scanner System *(MSS)*. At the ground receiving station, the *RBV* and *MSS* signals are processed and stored in digital form in computer-compatible tapes. Film transparencies of *RBV* and *MSS* images are produced using an Electron Beam Recorder *(EBR)*.

Although both the *RBV* and the *MSS* are basically line-scan systems, there are fundamental differences in the geometry of the scanning systems. At each *RBV* camera, an optical image of the scene is first focused on the photo-conductive target of the vidicon tube. The conductive property of the target converts the optical image into an electronic image, which is then scanned line-by-line by an electron beam. In the absence of any geometric distortions in the scanning system, an *RBV* image should possess all the central perspective properties of a conventional photographic image.

The *MSS* system optically scans the earth's suface line-by-line as the satellite travels along its orbit. The perspective center moves continuously along the orbital path, and the attitude of the satellite may also be continuously changing and thus affecting the orientation of each scan line. Consequently, an *MSS* image will not possess the central perspective properties. Basic descriptions of the *MSS* and *RBV* systems can be found in the *ERTS Data User's Handbook*.

Both the *RBV* and the *MSS* systems were designed primarily for remote sensing applications, rather than for cartographic mapping. Nevertheless, the geometric and cartographic accuracy of the two sensor systems are of vital importance to the success of the remote sensing experiments. Accurate geographic positions must be provided for whatever earth resources information are to be detected from the *RBV* and *MSS* data. Geometric fidelity will eventually affect the accuracy of quantitative analysis and measurement of earth resources, such as the com-

putation of areas and the detection of temporal changes by the correlation and comparison of sensor data.

The scale of the *RBV* and *MSS* images as well as the lack of good stereoscopic coverage ruled out the possibility of using these images for topographic mapping by stereophotogrammetric methods. However, because of the up-to-date coverage, the *RBV* and *MSS* images may be useful for updating small scale maps. The usefulness of the *RBV* and *MSS* images in cartographic mapping will depend largely on the resolution and geometric fidelity of the sensor systems.

Several investigators have reported in the literature both theoretical and experimental studies on the geometric and cartographic accuracy of *ERTS*-1 images. Colvocoresses (1970) estimated that the combined effects of earth curvature, camera tilt, topographic relief, atmospheric refraction and map projection error will result in geometric distortions amounting to less than ±50m at one sigma level. Kratky (1974) analyzed the geometric relationship of the *RBV* and *MSS* images with respect to the Universal Transverse Mercator *(UTM)* projection and concluded that the maximum discrepancy amounted to about ±60m for *RBV* images and ±125m for *MSS* images. Wong (1972) studied the geometric distortion characteristics in laboratory produced *RBV* pictures and found that the total geometric distortion from electronic sources amounted to ±463m and ±1,133m in the *X* and *Y* directions respectively with a resultant *RMS* distortion vector of ±1,224m. However, these experiments showed that the electronic distortions followed a systematic pattern and the random distortions amounted to only ±14m in the *X* and *Y* directions.

Colvocoresses and McEwen (1973) of the *USGS* reported that, based on analysis using photo-identified ground control points, the RMS distortion vectors in the bulk *MSS* images ranged from ±200m to ±450m. More recently, Schoonmaker (1974), also of the *USGS*, reported that the *RMS* distortion vectors in the bulk *MSS* images ranged from ±143 to ±279m. Schoonmaker based his analysis on 26 frames of *MSS* images from 11 different scenes covering three different locations along the Atlantic coast. However he measured only 7 to 16 photo-identified ground points in each *RBV* frame. The large variation in the magnitude of geometric distortions stated by Schoonmaker could be caused by instability of the *MSS* scanning system, instability of the *ERTS-1* attitude, or by the small number of control points used in each frame.

Derouchie and Forrest (1974) of Bendix Research Laboratories reported an experiment to determine the limiting geometric error in the *ERTS-1 MSS* system. Both optical and digital methods of identifying control points on the *MSS* images were tried. Polynomials of second and third degree as well as mathematically derived models were employed to model the geometric distortions. The limiting geometric distortion in the only *MSS* frame tested was found to be about ±60m.

This paper presents the results from a research study on the geometric and cartographic accuracy of the *RBV* and *MSS* images from *ERTS-1*. Four frames of bulk *RBV* images were analyzed using both the reseau images and photo-identified ground points. Two frames of *MSS* images were also analyzed using photo-identified ground control points. High-order polynomials were used to model the distortions in both the *RBV* and *MSS* images. The results provided an interesting comparison on the geometric fidelity and cartographic accuracy of the two sensor systems.

Polynomial Distortion Model

The following general polynomial model was used to model geometric distortions in both the *RBV* and *MSS* images:

$$\begin{aligned} &V_x + b_1 + b_2x + b_3y + b_4xy \\ &+ b_5x^2 + b_6y^2 + b_7x^2y + b_8y^2x \\ &+ b_9x^3 + b_{10}y^3 + b_{11}x^3y \\ &+ b_{12}y^3x + b_{13}x^4 + b_{14}y^4 + b_{15}x^2y^2 \\ &+ b_{16}x^3y^2 + b_{17}y^3x^2 + b_{18}x^5 \\ &+ b_{19}y^5 + b_{20}x^3y^3 = (x'_{calibrated} - x) \end{aligned} \quad (1)$$

$$\begin{aligned} &V_y + c_1 + c_2x + c_3y + c_4xy \\ &+ c_5x^2 + c_6y^2 + c_7x^2y + c_8y^2x \\ &+ c_9x^3 + \ldots + c_{20}x^3y^3 = (y_{calibrated} - y) \end{aligned} \quad (2)$$

where x and y are measured photo coordinates of an image point. A computer program (code-named PØLY20) was developed to determine the coefficients of a best-fitting polynomial for the x and y coordinates separately by the method of least squares. One or more terms of the polynomials could be held to zero in a solution, and the program also could compute the estimated standard errors of the computed coefficients. Thus the program could be used to model distortions with various degrees of polynomials; and from the standard errors of the computed coefficients, the insignificant terms in the polynomials

could be identified in the data output. Moreover, several frames of images could be used in a simultaneous solution to determine one pair of best-fitting polynomials for a large number of successive frames.

This polynomial model was initially developed to model the geometric distortions in television systems, such as the *RBV*. Its development was based on theoretical studies (Wong, 1967) which showed that the combined effects of all the sources of systematic distortions in a TV system could be described by a pair of high-order polynomials. The model had not been previously tested with *MSS* images, and the results obtained in this investigation were much better than could have been expected.

A review of the *MSS* distortion model developed by Kratky (1971) showed that the polynomial model was indeed theoretically valid for the *MSS* system. Kratky's mathematical model for *MSS* distortions took into consideration the effects of scanner geometry, panoramic effect, earth rotation, satellite orbit, satellite attitude, non-uniform scan rate and map projection. By using third-degree polynomials to describe the anomalies in satellite attitude, Kratky developed the following model for distortions in *MSS* images:

$$\begin{aligned}\Delta x = {} & (\frac{dX_o}{m} + f\phi_o) + x\,(\frac{dm}{m} + fb_1) \\ & + y\,\kappa_o + a_1xy + a_2x^2y + b_2x^2f \\ & + a_3x^3y + b_3x^3f;\end{aligned} \tag{3}$$

and

$$\begin{aligned}\Delta y = {} & \frac{dY_o}{m} - y\,\frac{dZ_o}{Z} \\ & + (f + \frac{y^2}{f})\,\omega_o + x\,(f + \frac{y^2}{f})\,c_1 \\ & + x^2\,(f + \frac{y^2}{f})\,c_2 \\ & + x^3\,(f + \frac{y^2}{f})\,c_3\end{aligned} \tag{4}$$

in which dX_o, dY_o are the corrections to the ground coordinates X, Y of a reference point in the *UTM* system, m is a scale factor; dm is the scale correction; Z is the flight sltitude; dZ is the correction to the flight altitude; f is the focal length; and x and y are image coordinates with the positive x-axis along the direction of flight. The attitude of the spacecraft was described by three rotation parameters ω, ϕ and κ as follows:

$$\begin{aligned}\omega &= \omega_o + c_1x + c_2x^2 + c_3x^3 \\ \phi &= \phi_o + b_1x + b_2x^2 + b_3x^3 \\ \kappa &= \kappa_o + a_1x + a_2x^2 + a_3x^3.\end{aligned} \tag{5}$$

Equation 3 may be rearranged:

$$\begin{aligned}\Delta x = {} & (\frac{dX_o}{m} + f\,\phi_o) + (\frac{dm}{m} + fb_1)x \\ & + \kappa_o y + a_1xy + a_2x^2y + (b_2f)x^2 \\ & + a_3x^3y + (b_3f)x^3;\end{aligned}$$

i.e.,

$$\begin{aligned}x = {} & g_o + g_1x + g_2y + g_3xy \\ & + g_4x^2 + g_5x^2y + g_6x^3 + g_7x^3y\end{aligned} \tag{6}$$

which is a polynomial of fourth degree. Similarly Equation 4 may be written:

$$\begin{aligned}\Delta y = {} & (\frac{dY_o}{m} + \omega_o f) + (c_1f)x - (\frac{dZ_o}{\Delta Z})y \\ & + (\frac{\omega_o}{f})y^2 + (c_2f)x^2 + (\frac{c_1}{f})xy^2 \\ & + (c_3f)x^3 + (\frac{c_2}{f})x^2y^2 + (\frac{c_3}{f})x^3y^2\end{aligned}$$

i.e.,

$$\begin{aligned}\Delta y = {} & h_o + h_1x + h_2y + h_3y^2 + h_4x^2 \\ & + h_5x^3 + h_6x^2y^2 + h_7x^3y^2\end{aligned} \tag{7}$$

which is a polynomial of fifth degree. All the terms in the polynomials of Equations 5 and 7 are also included in the 20-term polynomials expressed in Equations 1 and 2. The minor difference between Kratky's model and the general 20-term polynomials can be easily accounted for by the high-degree and correlation effects omitted in Kratky's derivation.

RBV System

The following four frames of *RBV* images from *ERTS-1* were used in the analysis: E-1003-16352-1, 2 and 3 and E-1003-18175-1. The first three frames were first-generation, 70-mm film transparencies having a nominal scale of 1:3,369,000 and were simultaneous exposures from the three *RBV* channels. The fourth frame (E-1003-18175-1) was a channel 1 exposure and was printed on a glass plate at the 1:1,000,000 scale (7.3 inch-by-7.3 inch image area).

GEOMETRIC ANALYSIS USING RESEAU

Every *RBV* camera tube has 81 reseau crosses etched permanently onto its photoconductive target. These reseau crosses are

TABLE 1. *RMS* DISTORTIONS CAUSED BY ELECTRONIC SOURCES IN THE *ERTS-1 RBV* IMAGES. (Based on Reseau Analysis)

Frame No.	*RMS* Distortions at Ground Scale (±Meters) Conformal Transformation			Affine Transformation			Std. Error in Coordinate Measurement at Ground Scale (±meters)	
	σ_x	σ_y	σ_r*	σ_x	σ_y	σ_r*	σ_x	σ_y
E-1003-16352-1	37	32	49	33	28	43	10	7
E-1003-16352-2	37	34	50	28	24	37	10	8
E-1003-16352-3	49	46	67	42	39	57	9	8
E-1003-18175-1	50	44	67	46	40	61	7	7
MEAN	43	39	58	37	33	50	9	8

*$\sigma_r = \pm\sqrt{\sigma_x^2 + \sigma_y^2}$

arranged in a square grid consisting of nine rows and nine columns. An image of this reseau appears in every frame of the *RBV* picture.

The image coordinates of the reseau crosses in the above four frames of *RBV* images were measured on a Wild STK-1 comparator, with two independent pointings to each reseau point. The calibrated coordinates of the reseau crosses were provided by the *USGS*. These calibrated coordinates were measured by the *USGS* as a part of the pre-flight calibration program, and were estimated to have an *RMS* error of $\pm 2\mu$m (McEwen, 1971).

The measured image coordinates were fitted to the calibrated coordinates using both conformal and affine transformations by the method of least-squares.

Table 1 lists the *RMS* distortions for each frame at ground scale. The estimated *RMS* errors contributed by the coordinate measurement process on the STK-1 comparator were also listed for each frame. The average *RMS* distortion vector (σ_r) for all four frames amounted to ±58m or 1.31 TV lines after conformal transformation. It represented the magnitude of geometric distortions caused by the electronic processes in the bulk *RBV* images. The coordinate measurement errors amounted to only ±12m at one sigma level. From previous experimental studies conducted with laboratory generated *RBV* images the *RMS* random distortions were found to be in the order of ±0.23 TV-lines in both the x and y directions, i.e., $\sigma_r = \pm 0.33$ TV lines. Thus, the total geometric distortions in these four frames were about four to five times larger than the expected random distortions. Figure 1 is a graphical plot of the residual distortion vectors in frame No. E-1003-16352-1 after conformal transformation. The distortion vectors appeared to follow a systematic pattern, which was almost identical in all four frames of *RBV* images.

GEOMETRIC ANALYSIS USING PHOTO-IDENTIFIED GROUND CONTROL POINTS

The three simultaneous exposures No. E1003-1635-1,2 and 3 were also used for geometric analysis by means of photo-identified ground control points. This *RBV* scene covered the area around Oklahoma City, Oklahoma. Control points were selected from 135 *USGS* topographic maps of the 1:24,000 scale. About one-third of the area had no 1:24,000 map coverage.

Fifty points of topographic and cultural features were identified on both the channel 2 frame and on the maps. Seven of these 50 points were later rejected in the data-processing phase because of poor identification and correlation. Among the 43 remaining ground points identified on the channel 2 frame, 27 points were also identified on the channel 1 frame and 21 points were identified in the channel 3 frame. During the coordinate measurement process, a 11X magnification was used on the viewing microscope. It was observed that the channel 2 (red) frame had much higher resolution and sharper images than the two frames from channels 1 (blue-green) and 3 (infrared). The drainage pattern, airport runways and two-lane highways could be easily identified on the channel 2 frame, but the identification was difficult in the other two frames.

The image coordinates of the ground points together with the 81 reseau points in each frame were measured on a STK-1 comparator. Four pointings were made to each point. The corresponding ground coordinates were measured on the 1:24,000 maps in the Oklahoma State Plane coordinate system, which was based on a Lambert Conformal map projection.

THREE-DIMENSIONAL PROJECTIVE TRANSFORMATION

The measured image coordinates of the ground control points were first fitted to the

corresponding ground coordinates by the method of three-dimensional projective transformation. In each computer solution, the interior orientation parameters (x_p, y_p and f) of the *RBV* camera were weighted with a standard error of ±0.001 mm at the values determined from preflight calibration. The ground coordinates of the control points were transformed into a local space rectangular coordinate system and the three coordinates (X_j, Y_j, Z_j) of each ground point were weighted with a standard error of ±1 m; i.e., $\sigma_X = \sigma_Y = \sigma_Z = \pm 1m$. The image coordinates were assigned relatively large standard errors in the solution ($\sigma_x = \sigma_y = \pm 0.500\ mm$), while the exterior orientation parameters were treated as completely unknown.

Table 2 presents a summary of the adjustment results. Two separate adjustments were made for each of the three frames. In one adjustment, the measured image coordinates were first corrected for electronic distortions using the reseau. The 20-term polynomials in Equations 1 and 2 were used to model the electronic distortions at the reseau points, and the same polynomials were subsequently used to apply corrections to the image coordinates of the ground control points.

The resulting average *RMS* distortion vector (σ_r) for the three frames amounted to ±90 m at ground scale. These residual distortions were caused by optical lens distortions, photographic processing, point identification and correlation errors, and errors in the measurement of both image and map coordinates.

Figure 2 is a graphical plot of the residual distortion vectors at the photo-identified ground points for the channel 2 frame when corrections for electronic distortions were applied. The plot did not display any significant systematic distortion pattern over the entire photograph.

In the second adjustment, no attempt was made to model and correct for electronic distortions. The resulting average *RMS* distortion vectors in the three frames amounted to

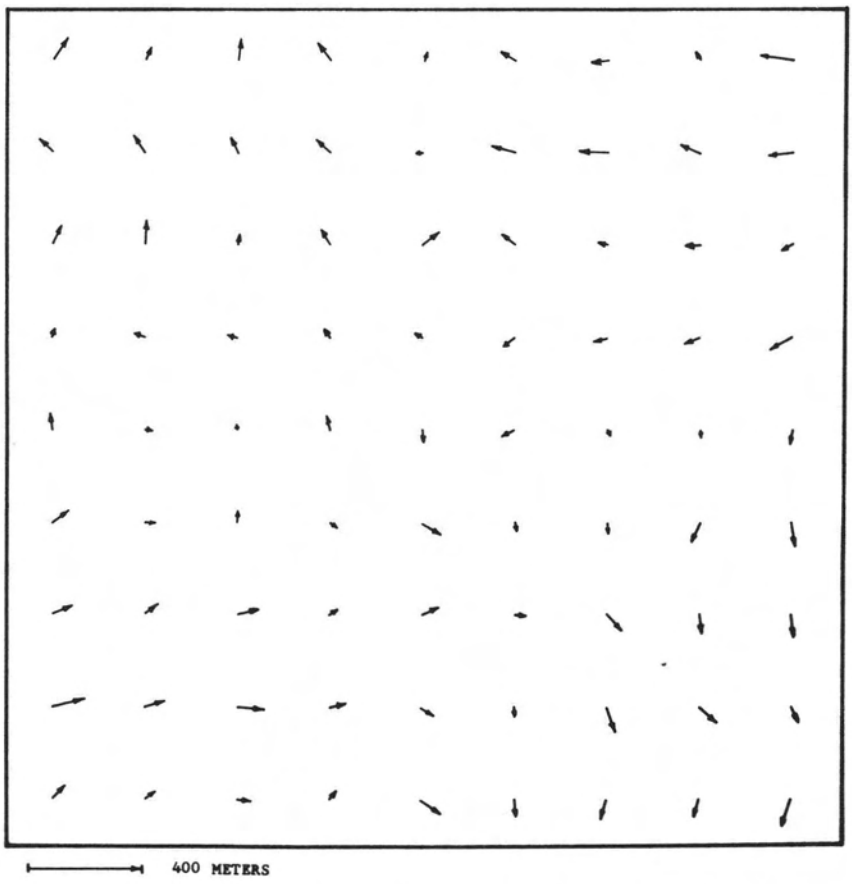

FIG. 1. Mean distortion plot conformal E-1003-16352-1 *RBV* PO 6555.

TABLE 2. *RMS* DISTORTIONS IN *RBV* IMAGES AFTER THREE-DIMENSIONAL PROJECTIVE TRANSFORMATION.

RMS Distortion	Corrections Applied for Electronic Distortions				No Corrections Applied for Electronic Distortions			
	Channel 1	Channel 2	Channel 3	Mean	Channel 1	Channel 2	Channel 3	Mean
σ_x (±meters)	55	71	43	56	65	81	75	73
σ_y (±meters)	68	78	62	69	84	81	88	84
σ_r (±meters)	88	107	75	90	107	114	114	110
No. of Control Points	27	43	21		27	43	21	

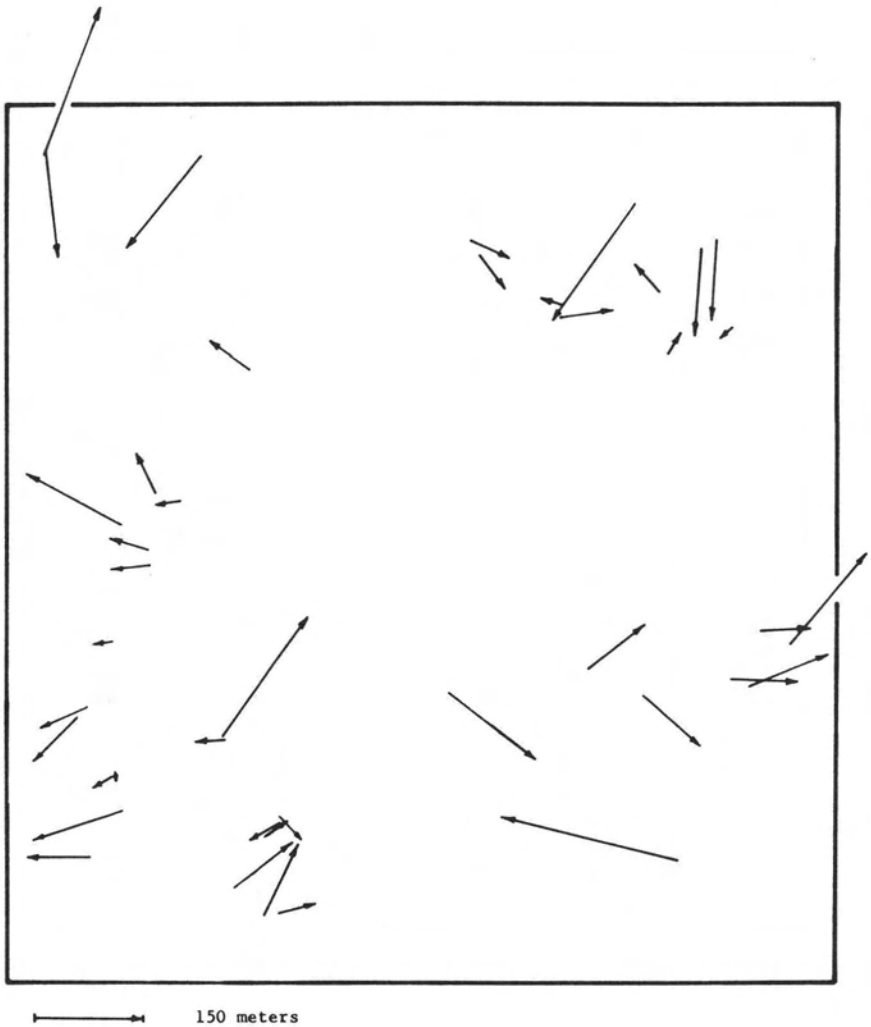

FIG. 2. Residual distortion vectors at the photo-identified ground points from in-flight calibration — *RBV* frame no. E-1003-1635-2 (electronic distortions were corrected from reseau measurements).

±110 m, which represented the total geometric distortions caused by electronic sources, optical lens distortions, errors in point identification and correlation, and errors in coordinate measurements.

TWO-DIMENSIONAL TRANSFORMATION

The magnitude of geometric distortions caused by earth curvature and map projection was investigated by fitting the image coordinates of the ground control points directly onto their corresponding State Plane coordinates. The methods of two dimensional conformal and affine transformations were employed. Since scene No. E-1003-1635-2 covered areas from both the Central and South zones of the Oklahoma State Plane Coordinate System, only the control points which were located in the Central zone was used in this analysis.

As in the case of three-dimensional projective transformation, two separate adjustments were performed for each photograph and each type of transformation. In one adjustment, the measured image coordinates of the ground points were corrected for electronic distortion using the reseau. In the second adjustment, no such correction was applied.

The results are summarized in Tables 3 and 4. The average *RMS* distortion vector (σ_r) after conformal transformation using uncorrected image coordinates was ±131m. This represented the internal cartographic accuracy of the *RBV* image. When corrections for electronic distortions were applied to the image coordinates, the mean *RMS* distortion vector after conformal transformation was reduced to ±105 m. It represented the limiting cartographic accuracy of the bulk images from the present *RBV-EBR* system, assuming that the correction procedure in the *EBR* could be improved to eliminate all constant components of electronic distortions.

The mean *RMS* distortion vectors after affine transformation was ±100 m with electronic corrections and ±113 m without corrections. These results showed that the photo-identified ground control points clearly detected the relative scale distortions in the x and y directions. When there was no correction applied for electronic distortions, the *RMS* distortion vector was reduced from

TABLE 3. RMS DISTORTIONS IN RBV IMAGES AFTER TWO-DIMENSIONAL CONFORMAL TRANSFORMATION.

RMS Distortion	Corections Applied for Electronic Distortions				No Corrections Applied for Electronic Distortions			
	Channel 1	Channel 2	Channel 3	Mean	Channel 1	Channel 2	Channel 3	Mean
σ_x (±meters)	69	69	72	70	80	81	92	84
σ_y (±meters)	82	79	69	77	97	83	121	100
σ_r (±meters)	107	108	100	105	126	116	152	131
No. of Control Points	10	30	13		10	30	13	

TABLE 4. *RMS* DISTORTIONS IN *RBV* IMAGES AFTER TWO-DIMENSIONAL AFFINE TRANSFORMATION.

RMS Distortions	Corrections Applied for Electronic Distortions				No Corrections Applied for Electronic Distortions			
	Channel 1	Channel 2	Channel 3	Mean	Channel 1	Channel 2	Channel 3	Mean
σ_x (±meters)	65	67	75	70	80	81	92	84
σ_y (±meters)	74	76	62	77	97	83	121	100
σ_r (±meters)	98	104	97	105	126	116	152	131
No. of Control Points	10	30	13		10	30	13	

±131 m for conformal transformation to ±113 m for affine transformation. When electronic corrections were applied, the relative scale distortions were corrected and the *RMS* distortion vectors were basically the same after both conformal and affine transformations.

The magnitude of the geometric distortions caused by the combined effect of map projection, non-verticality of the optical axis of the *RBV* camera and topographic relief can be estimated by comparing the results from two-dimensional conformal transformations to those obtained from three-dimensional projective transformation. For the cases in which the measured image coordinates were corrected for electronic distortions, the RMS distortion vectors obtained for the two types of transformation were as follows:

two-dimensional conformal transformation: $\sigma_r = \pm 105$ m

three-dimensional projective transformation: $\sigma_r = \pm 90$ m

Thus the geometric distortions (σ_g) caused by the combined effects of map projection, non-verticality and topographic relief can be computed:

$$\sigma_g = \pm \sqrt{(105)^2 - (90)^2} = \pm 54 \text{ m}.$$

REGISTRATION ANALYSIS

The mean RMS mis-registration vectors at the nine ground points which were identified on all three *RBV* photographs amounted to ±33 m, which included the combined effects of random electronic distortions, random errors in identifying the same point on all three frames, and random errors in coordinate measurements.

MSS System

MSS FRAME NO. E-1202-16381-4

A 70-mm film transparency of *MSS* frame No. E-1202-16381-4 was first analyzed. The frame was collected from channel 4 of the MSS on January 10, 1973 over the St. Cloud, Minnesota area.

One hundred eighty-nine (189) ground points were identified in both the 70-mm frame and on the available 1:24,000 *USGS* topographic maps of the area. These ground points included highway intersections, water features such as rivers and lakes, corners of woodlands, and water-land boundaries. The ice and snow cover in this winter scene greatly enhanced the boundaries between land and water as well as between woodland and open field. Similar experience was reported by Schoonmaker (1974), who further noted that the land-water interfaces were not sharp and were difficult to identify on summer scenes collected through channel 4.

The image points on the MSS frame were measured on a STK-1 comparator, with four pointings being made to each image point. The average standard deviation in each pointing was ±4 μm in x and ±5μm in y at frame scale, corresponding to ±14 m in x and ±17 m in y at ground scale. Both the Universal Transverse Mercator *(UTM)* and the Minnesota State Plane coordinates of these points were measured from the 1:24,000 maps.

TABLE 5. RESIDUAL *RMS* DISTORTION VECTORS IN FRAME NO. E-1202-16381-4.

Cases	σ_x (±meters)	σ_y (±meters)	σ_r* (±meters)	No. of Control Points
1. *UTM* Conformal	215	195	290	181
2. *UTM* Affine	148	114	187	181
3. State Plane Conformal	202	168	263	162
4. State Plane Affine	145	111	183	162
5. *UTM* 20-term Polynomials	37	44	57	181
6. *UTM* x (9 terms) y (8 terms)	44	54	70	181
7. *UTM* x (7 terms) y (8 terms)	44	54	70	181
8. *UTM* x (7 terms) y (5 terms)	44	74	86	181
9. *UTM* x (3 terms) y (3 terms)	94	67	115	181

*$\sigma_r = \pm \sqrt{\sigma_x^2 + \sigma_y^2}$

FIG. 3. Distortion map from conformal transformation to State Plane coordinates frame E-1202-16381-4.

Geometric distortions were computed by fitting the image coordinates to the ground coordinates using two-dimensional conformal and affine transformations. The program PØLY20 was used to model the distortions using polynomials of various degrees.

Table 5 presents a summary of the analysis results. In cases 1 and 2, distortion analysis was performed using *UTM* ground coordinates. The *RMS* distortion vectors were ±290 m and ±187 m after conformal and affine transformations respectively. In cases 3 and 4, analysis was performed using State Plane coordinates (Lambert Conformal Projection, Central Zone). The *RMS* distortion vectors were ±263 m and ±183 m after conformal and affine transformation respectively. Although the MSS image appeared to fit the State Plane coordinates slightly better than the *UTM* coordinates, the differences in the residual *RMS* distortions were negligibly small, especially after differential scale correction (affine transformation). Figure 3 is a graphical plot of the residual distortion vectors after conformal transformations to the State Plane coordinate system. The distortion vectors clearly displayed a systematic pattern.

While 181 points were used in the *UTM* cases, only 162 of these were used in the cases involving State Plane coordinates. The remaining 19 points were located in a different zone (South) of the State Plane coordinate system and therefore could not be used with the other 162 points which were located in the Central zone.

In cases 5 to 9, polynomials of various degrees were used to model the geometric distortions. The smallest *RMS* residual distortion vector (±57 m) was obtained with a pair of 20-term polynomials in case 5. Since the program PØLY20 also computed the estimated standard errors of the coefficients of the best-fitting polynomials, the least significant terms in the polynomials could be identified by their large standard errors. The

results in cases 6, 7, and 8 show that a major component of the systematic distortion can be modeled with a pair of polynomials consisting of seven to eight terms. The following polynomials were used in case 8:

$$r_x = b_2x + b_3y + b_4xy + b_8xy^2 + b_9x^3 + b_{10}y^3 + b_{13}x^4$$

$$r_y = c_1 + c_2x + c_3y + c_4xy + c_8xy^2 + c_9x^3 + c_{10}y^3 + c_{19}y^5$$

where x and y are measured image coordinates with respect to the comparator coordinate system (positive x and y axes are approximately in the East and North direction respectively); and r_x *and* r_y are the residual distortions.

The following first-degree polynomials were used in case 9:

$$r_x = b_1 + b_2x + b_3y$$

$$r_y = c_1 + c_2x + c_3y$$

This linear model is also sometimes referred to as six-parameter fit. In cartographic applications, this type of linear correction can be applied indirectly by varying the position of the grid lines for the *UTM* projection. The grid lines may be tilted and shifted laterally to compensate for the image distortion. The north-south grid lines may not be perfectly perpendicular to the east-west grid lines, and the scales may be slightly different along these two perpendicular directions; but the grid system will remain as straight lines. The residual *RMS* distortion vector for this case amounted to ±115 m, indicating that such a procedure might provide sufficient positional accuracy for 1:500,000-scale maps.

MSS FRAME NO. E 1394-16042-5

A 7.3-inch by 7.3-inch film transparency of MSS scene No. E-1394-16042-5 was also studied for geometric distortions. The image was collected from channel 5 of the *MSS* system and was dated August 21, 1973. The frame covered the central western part of Illinois and the eastern part of Indiana including the cities of Decatur, Champaign, Paris, Danville, Kankakee and West Lafayette. About three-fourths of the image was in Illinois. This part of Illinois was well covered with 1:62,000-scale USGS topographic maps. Many of these maps were dated before 1950 and and most of them did not include a *UTM* coordinate grid system. However, the dense network of secondary roads and their rectangular pattern made these linear features highly suitable as ground controls. Due to the sparse coverage of 1:24,000 maps in this area, 1:62,000 maps were used extensively to derive ground control coordinates.

The part of Indiana that was included in the frame had complete 1:24,000-scale map coverage, but had a different map projection coordinate system from the Illinois area. Because of the lack of a common ground coordinate reference system, no image point located within the Indiana area was measured.

The image coordinates of 70 photo-identified ground features were measured on a STK-1 comparator. The corresponding Illinois State Plane coordinates (East Zone, Transverse Mercator Projection) of these same points were measured from existing USGS maps.

Table 6 presents a summary of the geometric analysis performed on this frame. The residual *RMS* distortion vector was ±347m for both two-dimensional conformal (case 1) and affine transformation (case 2). Thus, the magnitude of geometric distortion on this frame was considerably larger than that found in frame No. E-1202-16381-4.

Figure 4 is a graphical plot of the residual distortion vectors after conformal transformation. By comparing Figure 4 with Figure 3, it is obvious that the distortion pattern in frame No. E1394-16042-5 differed significantly from that of frame No. E-1202-16381-4. Such a major difference in distortion pattern could be caused by a combination of factors including instability of the *MSS* system, variation in the sensor's attitude and engineering modification or adjustment which could have been performed on the ground equipment during the eight-month interval between the collection of the two frames.

In cases 3 to 6 in Table 6, polynomials of various degrees were used to model the geometric distortions. Although the distortion pattern was significantly different, the *RMS* residual distortions for these cases were almost identical in magnitude to those found in frame No. E-1202-16381-4 which were given in Table 5. When a pair of 20-term polynomials was used as distortion model, the residual RMS distortion vector amounted to only ±53 m, as compared to ±57 m in frame No. E-1202-16381-4. The *RMS* distortion vectors were increased to ±67 m and ±100 m for the cases using 8-term and 3-term polynomials respectively. The 3-term polynomials in case 6 included only first-degree terms.

CARTOGRAPHIC ACCURACY

Table 7 summarizes the test cases which can be used to evaluate the cartographic ac-

TABLE 6. RESIDUAL *RMS* DISTORTION VECTORS IN FRAME NO. E-1394-16042-5

Cases**	σ_x (±meters)	σ_y (±meters)	σ_r* (±meters)	No. of Control Points
1. Conformal	222	267	347	64
2. Affine	222	267	347	64
3. 20-term Polynomials	25	47	53	64
4. x (10 terms) y (11 terms)	41	47	62	64
5. x (8 terms y (8 terms)	49	46	67	64
6. x (3 terms) y (3 terms)	74	67	100	64

*$\sigma_r = \pm\sqrt{\sigma_x^2 + \sigma_y^2}$
** Illinois State Plane Coordinates (East Zone) were used in all cases.

curacy of the *ERTS-1 RBV* and *MSS* systems. The *RMS* distortions are expressed both at ground scale and at three different map scales: 1:1,000,000; 1:500,000; and 1:250,000. The National Map Accuracy Standards (NMAS) require that for maps which have a scale smaller than 1:20,000 not more than 10 per cent of the well-defined points that are tested should have positional error exceeding 1/50 of an inch. In order to meet this requirement, the *RMS* distortion vector (σ_r) at map scale must be less than or equal to ±0.310mm for maps at scale smaller than 1:20,000.

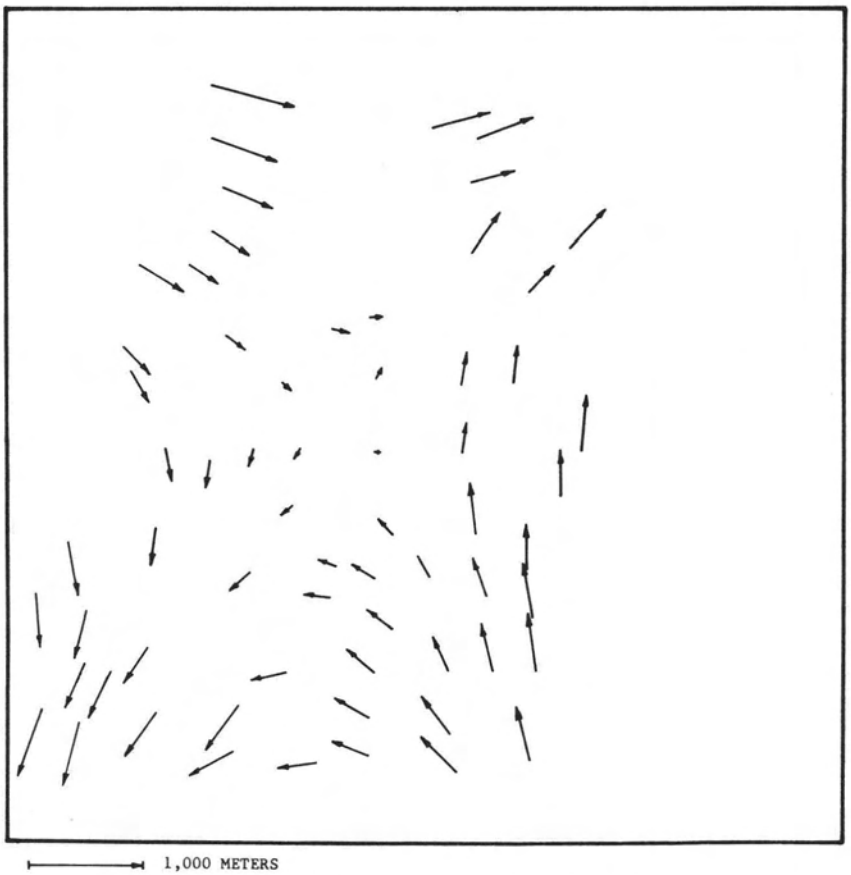

FIG. 4. Distortion map from conformal transformation to State Plane coordinates frame no. E-1394-16042-5.

Case 1 in Table 7 showed that the *RMS* distortion vector in the *ERTS/1 RBV* images amounted to only ±58 m, which is equivalent to ±0.232mm at the 1:250,000 map scale. Thus, the bulk *RBV* images from *ERTS*-1 had sufficient geometric fidelity to meet the NMAS for 1:250,000 scale mapping. However, due to the relatively low resolution capability of the *RBV* system, positioning error of considerable magnitude is introduced in the process of correlating a photo-identified point with its corresponding point in the existing topographic maps. Case 2 showed that including the errors introduced in point identification, correlation and measurement, the expected *RMS* error in geographic positioning from *RBV* data amounted to ±90 m. Case 3 showed that the effects of map projection, topographic relief, earth curvature and non-verticality of the camera axis further degraded the cartographic accuracy of the bulk *RBV* image to ±131 m, which is equivalent to ±0.262 mm in a 1:500,000 map sheet. Thus, without any further processing, the bulk *RBV* images should have sufficient geometric fidelity to meet the NMAS requirement for 1:500,000 scale mapping.

Although the *ERTS-1 RBV* system has sufficient geometric fidelity for 1:250,000 mapping, it is unlikely that the system has sufficient resolution to provide the details needed for mapping at that scale. Unfortunately, the *RBV* television system was turned off shortly after *ERTS-1* was in orbit. Since the electronic distortions in the *RBV* bulk images, as shown in Figure 2, displayed a systematic pattern, it is quite likely that the distortion correction process in the *EBR* output system could be further improved to reduce the *RMS* distortions to under ±40 m. It is also probable that had the *RBV* system been allowed to operate continuously, some engineering adjustments could have been made to improve the system resolution.

Cases 4 and 5 in Table 7 showed that the *MSS* bulk images from *ERTS-1* did not have sufficient geometric accuracy to meet the NMAS requirement for mapping at 1:1,000,000 scale. However, cases 6 and 7 showed that by applying geometric corrections with a pair of linear polynomials, the magnitude of geometric distortions could be reduced to about ±110 m, which would meet the accuracy requirement for 1:500,000 scale mapping. A minimum of four and perhaps as many as eight to ten ground control points will be required to determine the coefficients of the linear polynomials for an *MSS* frame.

Cases 8 and 9 showed that by modeling the system distortions with a pair of 20-term polynomials, the residual distortion vectors after geometric correction could be reduced

TABLE 7. CARTOGRAPHIC ACCURACY OF THE *ERTS-1 RBV* AND *MSS* IMAGES.

Cases	*RMS* Distortion at Ground Scale			*RMS* Distortion Vector (σ_r) at Map Scale		
	σ_x (East)	σ_y (North)	σ_r	1:1,000,000	1:500,000	1:250,000
1. *RBV* Electronic Distortions	±40 m	±40 m	±58 m	±0.058 mm	±0.116 mm	±0.232 mm
2. *RBV* Geographic Positioning Accuracy	56 m	69 m	90 m	0.090 mm	0.180 mm	0.360 mm
3. *RBV* Bulk Image Cartographic Accuracy	84	100	131	0.131	0.262	0.524
4. *MSS*/Total Distortion as compared to *UTM* Coordinates (E-1202-16381-4)	215	195	290	0.290	0.580	1.160
5. *MSS*/Total Distortion as compared to State Plane Coordinate (E-1394-16042-5)	222	267	347	0.347	0.694	1.388
6. *MSS*/After Correction with first-degree polynomials equivalent to grid fitted accuracy (E-1202-16381-4)	94	67	115	0.115	0.230	0.460
7. *MSS*/After Correction with first-degree polynomials (E-1394-16042-5)	74	67	100	0.100	0.200	0.400
8. *MSS*/After Correction with 20-term polynomials (E-1202-16381-4)	37	44	57	0.057	0.114	0.228
9. *MSS*/After Correction with 20-term polynomials (E-1394-16042-5)	25	47	53	0.053	0.106	0.212

to ±55 m, which was sufficiently accurate for 1:250,000 maps. However, at least 20 ground control points per frame would be required for the determination of the 20-term polynomial and about 30 ground points would be required in practice to provide a reasonable degree of redundancy in the least-squares solution.

RBV Reseau

The *RBV* reseau has served two important functions in the *ERTS-1* program: (1) it was used as a target field for the determination of the focal length, the position of the principal point in the image plane, and the lens distortion characteristics in pre-flight calibration (McEwen, 1971), (Wong, 1973); and (2) it provided a net of reference targets which could be used for the accurate calibration of electronic distortions in both pre-flight and in-flight calibration. Both the CBS Electron Beam Recorder (EBR) and the Bendix Precision Processor depend on the reseau to derive accurate distortion patterns for geometric correction.

However, the reseau presents an undesirable obstruction to the user of *ERTS* images in interpretation tasks. Valuable image information may sometimes be masked by the reseau crosses. There is a genuine need therefore to eliminate completely either the reseau or to reduce the number of reseau crosses.

The experimental results discussed have shown that photo-identified ground control points could be used to calibrate the total geometric distortions in the entire *RBV* system. By choosing a *RBV* scene which is 100 per cent cloud free and which covers an area that is well covered with 1:24,000 or 1:62,500 maps, literally hundreds of ground points can be identified on both the *RBV* image and the map. The geographic position of the ground points can be derived directly from the existing maps, and the image coordinates of the same points in the *RBV* image can be accurately measured on a comparator. Then, based on the projective relationship between the image and the ground, the total *RBV* geometric distortion at each image point can be determined using a least-squares adjustment procedure. Alternatively, the image coordinates can be fitted to map projection coordinates of the ground points; and the computed distortions will include the effects of map projection distortions.

The accuracy of distortion calibration using photo-identified ground control points depends on the accuracy of correlating an image point on the *RBV* scene to the corresponding point in the map. The accuracy of correlation in turn depends on the resolution of the *RBV* system. It was found from this investigation that the total *RMS* error of point identification, correlation and coordinate measurements could amount to ±70m when visual methods were used. This method of geometric calibration should be sufficiently accurate to control the *RBV* distortions to within ±110 m.

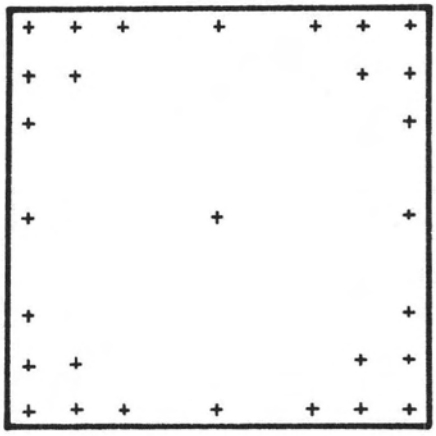

FIG. 5. A 29-point reseau pattern.

Since the *RBV* distortions followed a highly systematic pattern, it could be expected that the distortion pattern can be modeled with considerably fewer than 81 reseau points. Figure 5 shows a 29 point reseau pattern that was tested for its effectiveness in modeling the distortion pattern. These 29 points were selected from the present 81-point pattern to closely resemble a 31-point reseau pattern proposed by McEwen of the *USGS* (McEwen, 1972). Ten frames of laboratory photographs from an experimental *RBV* system were used in the analysis.

The calibrated coordinates of the 29 reseau points were used with the corresponding measured image coordinates to determine the coefficients of the distortion polynomials. These polynomials were then used to apply distortion corrections to the measured image coordinates of the 52 check points. Then, the corrected coordinates of these check points were compared with their calibrated coordinates to evaluate the accuracy of distortion modeling and correction by polynomials.

Two separate approaches were attempted. In the first approach, the distortions at the 29 reseau points were modeled with a pair of 20-term polynomials for each frame individually. In each frame, the measured coordinates of the 52 check points were corrected

with the polynomials derived from the 29 reseau points in that frame.

In the second approach, all 10 frames were used simultaneously to determine the best-fitting polynomials for all 10 frames. The measured coordinates of the check points in all 10 frames were then corrected with the same pair of polynomials.

The mean *RMS* distortion vector at the 52 check points amounted to ±1,005 m. After correction using separate polynomials for individual frames the mean *RMS* distortion vector was reduced to ±78 m. Almost identical residuals (±79m) were obtained when distortions were modeled with a pair of best-fitting polynomials for all 10 frames. It was evident that the 29-point reseau pattern would be quite effective in controlling the geometric fidelity of the *RBV* system when used in conjunction with the polynomial distortion model.

A 25-point reseau, consisting of five symmetrical rows and columns, was also tested using the same technique; but the polynomial model was found to be totally ineffective for such a reseau pattern.

Conclusions

Both the *RBV* and *MSS* systems have merits and demerits in cartographic applications. The geometric fidelity of the *RBV* system is excellent. Electronic distortions in the *RBV* system amounted to only ±58m. However, its low resolution reduced the geographic positioning accuracy for well defined ground features to ±90m. With three or four photo-identified ground control points for each frame, the bulk *RBV* images should have sufficient geometric accuracy to meet the NMAS requirement for mapping at 1:500,000 scale.

In order to make the *RBV* images more attractive as a cartographic product, a new reseau pattern should be developed to replace the 81-point pattern being used in *ERTS-1*. The dimensions of the reseau crosses should be reduced, and the crosses should be located near the edges and corners of the frame. Serious consideration should also be given to replacing the reseau crosses with circular dots such as those used in the television systems of the *Surveyor* spacecrafts (Wong, 1970).

The geometric fidelity of the *MSS* system is considerably inferior to that of the *RMV* system. the *RMS* distortion vectors in a bulk *MSS* image may range from ±150 to ±350m. However, the distortion is highly systematic, and by using four or more photo-identified control points, an *MSS* image can be corrected to meet the NMAS requirement for mapping at 1:500,000 scale.

In the digital processing of *RBV* and *MSS* data from *ERTS-1*, a relative geographic positioning accuracy of ±55m should be attainable. Since *RBV* frame has an internal geometric accuracy approaching ±55m, only three to four ground control points are needed to orient the *RBV* frame to a geographical reference. However, the *MSS* distortions are primarily caused by irregular variations in the attitude of the satellite. Since the pattern of variation differs from frame-to-frame, the limiting accuracy of ±55m can only be achieved by the accurate calibration of each frame using as many as 25 to 30 ground control points.

In spite of the highly promising results that have been obtained in geometric analysis, the usefulness of *RBV* and *MSS* images in cartographic applications is severely limited by the low resolution, lack of stereoscopic coverage and the small scale of the images. There were times during this investigation when even major features such as highways, dams and perennial streams could not be consistently identified on the *MSS* and *RBV* images. The identification of ground features depended on object size, scene contrast, orientation of the feature with respect to the scan lines as well as the spectral response characteristics of the sensors. A serious study should be conducted to evaluate the information content and resolution limitation of the *RBV* and *MSS* images with respect to the information content generally required for mapping at the scales of 1:1,000,000, 1:500,000 and 1:250,000.

Acknowledgment

The work reported in the paper was supported by the U. S. Department of the Interior, Geological Survey. The technical support provided by Dr. Robert McEwen of the Geological Survey is gratefully acknowledged.

References

1. Colvocoresses, A. P.; ERTS-A Satellite Image, *Photogrammetric Engineering*, Vol. 36, No. 6, June 1970, pp. 555-560.
2. Colvocoresses, A. P.; McEwen, R. B.; EROS Cartographic Progress, *Photogrammetric Engineering*, Vol. 39, No. 12, December 1973, pp. 1303-1309.
3. Derouchie, William F.; Forrest, R. E.; Potential Positioning Accuracy of ERTS-1 MSS Images, a paper presented at the 1974 ACSM-ASP Convention, St. Louis, Missouri, March 10-15, 1974.

4. Kratky, V.; Cartographic Accuracy of ERTS, *Photogrammetric Engineering*, Vol. 40, No. 2, February 1974, pp. 203-212.

5. McEwen, Robert B.; Geometric Calibration of the RBV System for ERTS, *Proceedings of the 7th International Symposium on Remote Sensing of Environment*, May 17-21, 1971, The University of Michigan, Ann Arbor, Michigan.

6. McEwen, Robert B.; Suggested RBV Reseau Pattern, USGS Memorandum for the Record (EC-5-ERTS), October16, 1972.

7. NASA Goddard Space Flight Center, *Earth Resources Technology Satellite Data User's Handbook*, Document No. 71SD4249.

8. Schoonmaker, James W. Jr.; Geometric Evaluation of MSS Images from ERTS-1, Proceedings of the ASP 40th Annual Meeting, St. Louis, Missouri, March 10-15, 1974; pp. 582-587.

9. Wong, K. W.; Fidelity of Space TV, *Photogrammetric Engineering*, Vol. 36, No. 5, May 1970, pp. 491-497.

10. Wong, K. W.; Geometric Analysis of the RBV Television System (Phase II), *Civil Engineering Studies*, Photogrammetry Series No. 35, University of Illinois at Urbana-Champaign, 1972.

11. Wong, K. W.; A Computer Program Package for the Geometric Analysis of ERTS-1 Images, *Civil Engineering Studies*, Photogrammetry Series No. 41, University of Illinois at Urbana-Champaign, June 1974.

Symposium on Close-Range Photogrammetric Systems

Champaign-Urbana, Illinois
July 28 - August 1, 1975

The Symposium on Close-Range Photogrammetric Systems, sponsored by the Close-Range Photogrammetry Committee and the Computational Photogrammetry Committee of the American Society of Photogrammetry in cooperation with ISP Commission V and the University of Illinois at Urbana-Champaign, will be held at the Ramada Inn Convention Center, 1501 South Neil Street, Champaign, Illinois 61820.

Session topics will include:

Architectural Applications
Engineering and Industrial Applications
Biostereometrics
Underwater Mapping Systems & Applications
Holographic and Microscopic Systems & Applications
Computational Procedures and Software (2 sessions)
Photogrammetric Equipment Systems
Manufacturers-Users Forum

A number of photogrammetric equipment manufacturers, government agencies (including the Naval Photographic Center) and universities will exhibit the latest equipment systems and other items pertaining to close-range photogrammetry.

Registration fees will be $30 for ASP members and $35 for non-members.

For information on the Symposium contact Dr. H. M. Karara, 3129 Civil Engineering Building, University of Illinois, Urbana, Illinois 61801. Tel: (217) 333-4311.